Journal of the European Ceramic Society **16** (1996) 695–702

0955-2219(95)00197-2
0955-2219/96/$15.00

Critical Notch-Root Radius Effect in SENB-S Fracture Toughness Testing

R. Damani, R. Gstrein & R. Danzer*

Christian Doppler Laboratorium für Hochleistungskeramik am Institut für Struktur- und Funktionskeramik, Montanuniversität Leoben, A-8700 Leoben, Austria

(Received 20 September 1995; revised version received 20 October 1995; accepted 30 October 1995)

Abstract

The brittle behaviour of ceramic materials makes imperative the development of accurate and reproducible methods of measuring their resistance to fracture. To this end, a European round robin was set up to investigate the relative merits of five different methods of fracture toughness testing. Of these the single edge notch bend – saw cut (SENB-S) method seemed to deliver the most reproducible results, both within and between laboratories. However, it has been observed empirically that if notches are cut too thick, the values of fracture toughness determined are systematically too high. An explanation and a theoretically based relationship to describe this behaviour are presented. It is suggested that this effect results from the interaction of the stress field around the notch tip and defects related to the microstructure or machining damage. Measured data from a number of materials seem to correlate well with the theory. It is shown that if correct values of fracture toughness are to be determined with the SENB-S method, the notch width must be of the order of the size of the relevant microstructural or machining-induced defects (e.g. large pores and weak grain boundaries).

Introduction

The greatest limitation in the use of ceramic materials for load-bearing applications is their brittleness. To overcome this problem tougher materials must be engineered. More accurate and reproducible methods of fracture toughness testing are required to enable an objective evaluation of the progress made in improving the resistance to crack propagation of ceramic materials.

With this in mind, The European Structural Integrity Society-Technical Committee 6 (ESIS TC6) set up a round robin to evaluate five commonly used methods of fracture toughness testing: the chevron-notched beam (CVN); the indentation fracture (IF); the indentation strength in four-point bending (IS); the single-edge precracked beam in four-point bending (SEPB–B) using popped in bridging cracks, and the single edge notch bend – saw cut (SENB-S) methods. The results of this round robin showed that the SENB-S method, although not always the most accurate, seems to be the most reproducible both within and between laboratories.[1] Furthermore, the SENB-S method requires very little specialized apparatus and specialist skill. It is therefore cheap and applicable in most standard mechanical laboratories. The major limiting feature of this method, however, is the appearance of a limiting *critical notch root radius*, above which the values of K_{Ic} determined are systematically too high. In this work an explanation is presented that relates the occurrence and magnitude of this critical notch root radius, ρ_c, to microstructural features of the ceramic material. A relationship that allows a first approximation of the magnitude of ρ_c is suggested.

Fracture Toughness Testing in Ceramics

A major problem of fracture toughness testing of ceramics is the difficulty in reliably introducing reproducible and easily measurable sharp cracks into the samples. In metals fatigue cracks are initiated and grown in a controlled manner, but this is too difficult, if not impossible, in ceramic samples. Various other methods have been devised to initiate such cracks in ceramic samples, e.g. by using the bridging method or a chevron-notched sample (where the initial cracks run into a field of decreasing stress intensity),[2] but they tend to produce long cracks that are difficult to measure and difficult to reproduce. In the SENB-S method most of these problems are avoided since it is relatively

*To whom correspondence should be addressed.

easy to machine an accurate notch, the exact depth of which is easily discernible in an optical microscope. The machined notch is then assumed to act as a long, sharp crack.

It should be noted that there are ceramic materials with more or less constant crack resistance, and other ceramic materials where the crack resistance increases as the crack grows. In the following analysis emphasis is placed on the first type of material.

The SENB-S Method and the Critical Notch Root Radius

The SENB-S method involves taking small-beam samples (typically of breadth b = 3 mm, height w = 4 mm and length L = 45 mm), sawing a suitable notch to a depth a_0 and then testing to fracture in four-point bending [see Figs 1(a) and 1(b)]. The depth of the notch is determined by optical analysis of the fractured surfaces. It is assumed that fracture initiates from some statistically distributed small flaw in front of the notch. The size of this flaw, δa, correlates with some microstructural feature. The total crack length at failure is then: $a_f = a_0 + \delta a$. However, since $\delta a << a_0$, and δa is difficult to find and measure, the approximation $a_f \approx a_0$ is usually applied. The stress at failure, σ_f, is used to calculate the critical stress intensity factor (i.e. the fracture toughness), K_{Ic}, from a relationship based on the standard linear elastic fracture mechanics relationship:

$$K_I = Y \sigma \sqrt{\pi a} \tag{1}$$

where Y is a correction factor allowing for the influence of sample geometry and crack configuration. The following relationship,[3] applicable to long, sharp crack configurations with values of α between 0·4 and 0·6, was used in the round robin investigation for calculating K_I:

$$K_I = \frac{F}{b\sqrt{w}} \frac{S_1 - S_2}{w} \frac{3\sqrt{\alpha}\, \Gamma_M}{2(1-\alpha)^{3/2}} \tag{2}$$

where

$$\Gamma_M = 1{\cdot}9887 - 1{\cdot}326\,\alpha - \frac{(3{\cdot}49 - 0{\cdot}68\,\alpha + 1{\cdot}35\,\alpha^2)\,\alpha\,(1-\alpha)}{(1+\alpha)^2}$$

$\alpha = a_f/w$, F is the load, and S_1 and S_2 are the outer and inner roller spans of the four-point bending fixture, respectively. The critical stress intensity factor K_{Ic} is obtained if the maximum load before failure, F_{max}, is used in eqn (2). (Note: If, for instance, w = 4 mm, a_0 = 2 mm, and δa = 50 μm the error made by applying the approximation $a_f \approx a_0$ in calculating K_{Ic} from eqn (2) is about 3·8%.)

The notches are typically cut to half the depth of the beam ($\alpha \approx 0{\cdot}5$). The half-width of the saw cut is taken to be the notch root radius, ρ.

It is commonly presented in literature[3–5] that, if the notches are too wide, i.e. the notch-root radius ρ is too large, the values of K_{Ic} will be systematically determined too high. Only below some critical value of notch-root radius ρ_c will the values of K_{Ic} remain constant and correct (Fig. 2). Indeed, some such behaviour is to be expected if the differences in stress distribution in front of a notch and in front of an infinitely sharp crack are considered and, in fact, is often observed empirically.

Thus, by treating the notch as a blunt crack and by considering the true role of small cracks at the notch tip, an explanation for this critical notch-root radius effect becomes evident. These small cracks can be assumed to be in-plane material

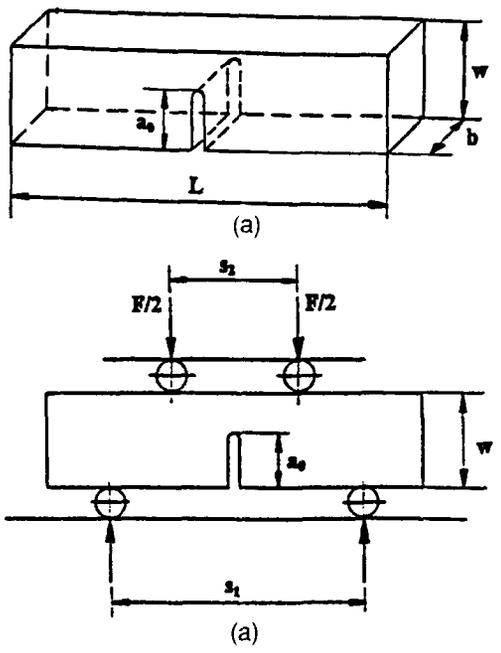

Fig. 1. (a) Geometry of edge-notched small beam sample; (b) schematic arrangement of sample in a four-point bend test.

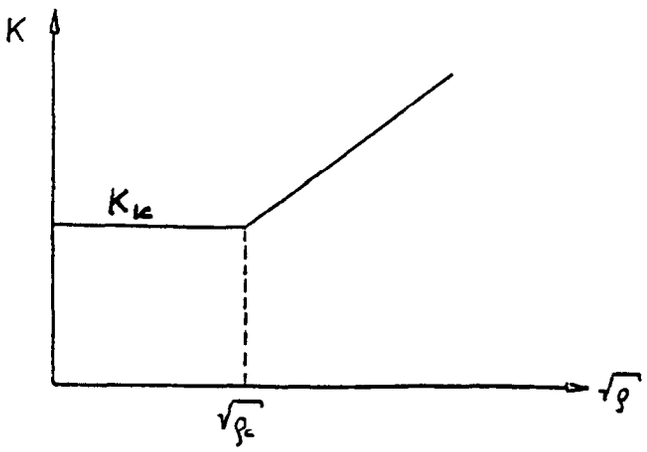

Fig. 2. Schematic representation of dependence of measured fracture toughness K_{Ic} on notch-root radius ρ (from Munz & Fett[3]).

flaws, or machining damage, statistically distributed along the notch front [Fig. 3(a)]. For analytical simplicity it is convenient to replace the true notch-crack configuration with an assumed idealized configuration, e.g. a through-thickness edge crack [Fig. 3(b)] or a half-penny crack [Fig. 3(c)]. The true configuration will be somewhere in between. The conventional concept of a long crack, i.e. $a_f \approx a_0$, in which the influence of the notch is neglected, may then be replaced by the configuration of a small crack in front of a notch, which lies in a stress field under the influence of the notch. In the following the ratios of the corresponding stress intensity factors are calculated.

By using a standard fracture mechanics approach to blunt cracks to calculate the notch tip stress,[6] and by re-applying (1) with the appropriate geometric correction factor (e.g. for a through-thickness edge crack $Y = 1{\cdot}12$ and for a half-penny shaped crack $Y \approx 2/\pi$), the ratio of the true stress intensity factor seen by a small notch-tip crack K_{ntc} to the stress intensity factor for long sharp cracks K_{lsc} calculated by (2) is given as

$$K_{ntc} / K_{lsc} \approx 2\ Y \sqrt{\delta a / \rho} \qquad (3)$$

This relationship is valid for very small cracks where $\delta a << \rho_c$ and may be applied as an approximation for small cracks. The stress intensity factor calculated from eqn (2), however, is valid for long cracks where $\delta a >> \rho_c$. The change in stress intensity as the fracture-initiating crack varies from short to long crack may be given by suitably weighting the two functions (2) and (3). To this end, Fett[7] suggested the following simple function

$$X \approx \tanh (2\ Y \sqrt{\delta a / \rho}) \qquad (4)$$

where

$$X = \frac{K_{ntc}}{K_{lsc}} \qquad (5)$$

(note that $\tanh x \approx x$ for $x << 1$, and $\tanh x \to 1$ as $x \to \infty$).

The validity of the above weighting function has been corroborated by applying the boundary collocation method. In Fig. 4(a) stress intensity is plotted against the relative notch depth α and small crack size δa. It shows schematically the curves of K for long cracks as obtained from eqn (2) and for small cracks according to eqn (3) in the area around the notch tip as functions of α and δa, respectively, when all other conditions are kept constant. The solid line shows the weighted function for K_{ntc} using eqn (4). Figure 4(b) shows the strong dependence of the weighted function on ρ.

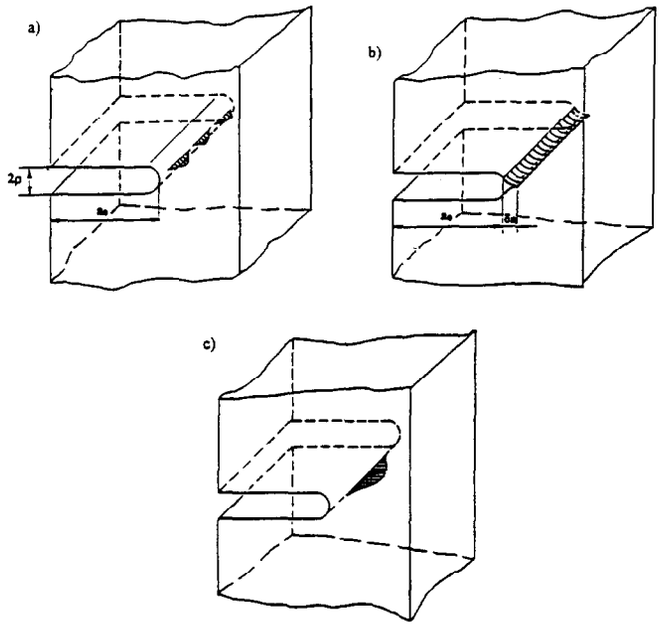

Fig. 3. (a) Schematic representation of notch and natural, in-plane notch-tip defects (true notch-crack configuration); (b) idealized edge-crack configuration; (c) idealized half-penny configuration.

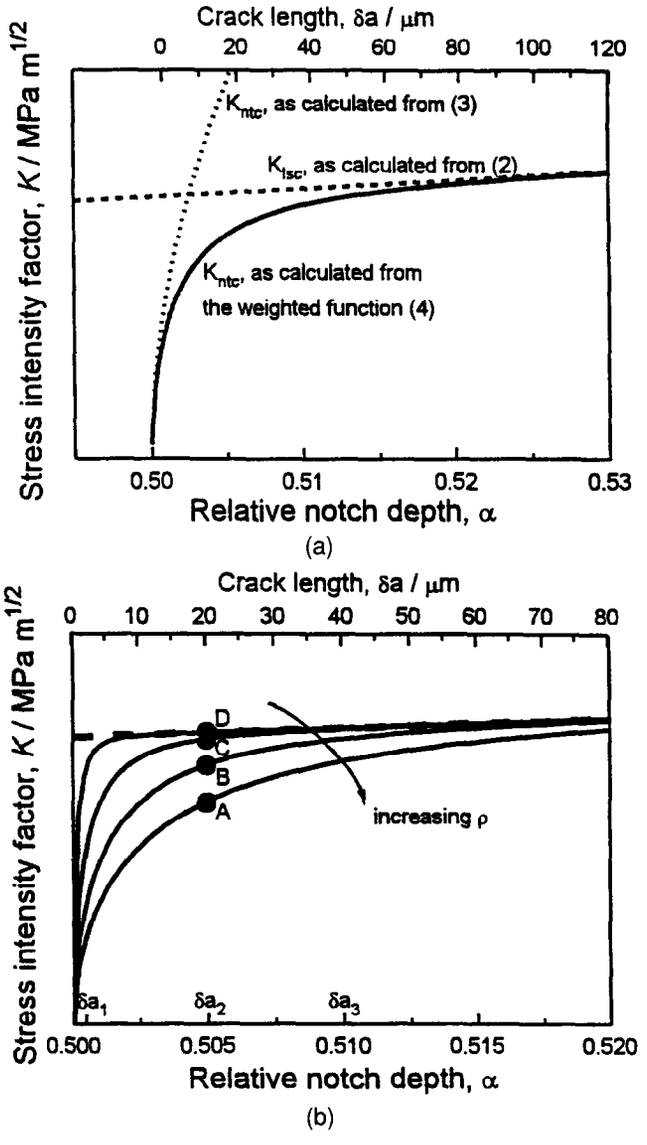

Fig. 4. (a) Stress intensity factors for long sharp cracks and small notch-tip cracks as calculated from eqns (2) and (3) respectively, and the weighted function, eqn (4). (b) Dependence of the weighted function (4) on notch-root radius ρ.

Points A, B, C and D mark the stress intensity factors that would be seen by a small crack of length δa_2 in front of the notch. The dashed line represents the K_{Ic} that would be calculated for long sharp cracks under the same conditions.

Figure 5(a) shows schematically the variation in K_{Ic} values determined from the notch-crack configurations suggested above, i.e. varying notch width and δa kept constant. The scatter bars give an idea of the magnitude of empirical scatter typically observed. Figure 5(b) shows schematically the types of curves that would be attained for three different small crack sizes, where $\delta a_1 < \delta a_2 < \delta a_3$, as shown in Fig. 4(b).

It can clearly be seen that small cracks in front of notches can actually experience significantly lower stress intensities than the corresponding long cracks, i.e. $K_{ntc} < K_{lsc}$ [see points A and B in Fig. 4(b)]. Bearing in mind that the ceramic materials considered behave in a predominantly brittle fashion and do not show increasing crack resistance as cracks grow, the small cracks will not grow before fracture occurs. Therefore, to initiate fast fracture from such a small crack, it is necessary to apply significantly higher forces, compared with a system with the corresponding long crack, before $K = K_{Ic}$ at the crack tip. Thus, assuming eqn (4) is correct, fracture toughness values calculated using eqn (2) would be higher than the true fracture toughness. How much higher depends on the magnitude of the effect of the notch and the size of the starting defect. Generally, the wider the notch the more force is required and the higher the value of K_{Ic} determined [see corresponding points A' and B' in Fig. 5(a)]. If, however, the notch is thin enough, the stress intensity at the tip of the small crack does not greatly differ from that seen by an equivalent long crack [see points C and D and dashed line in Fig. 4(b)]. Thus a correct value (within the scatter) of fracture toughness is measured [see corresponding points C' and D' in Fig. 5(a)].

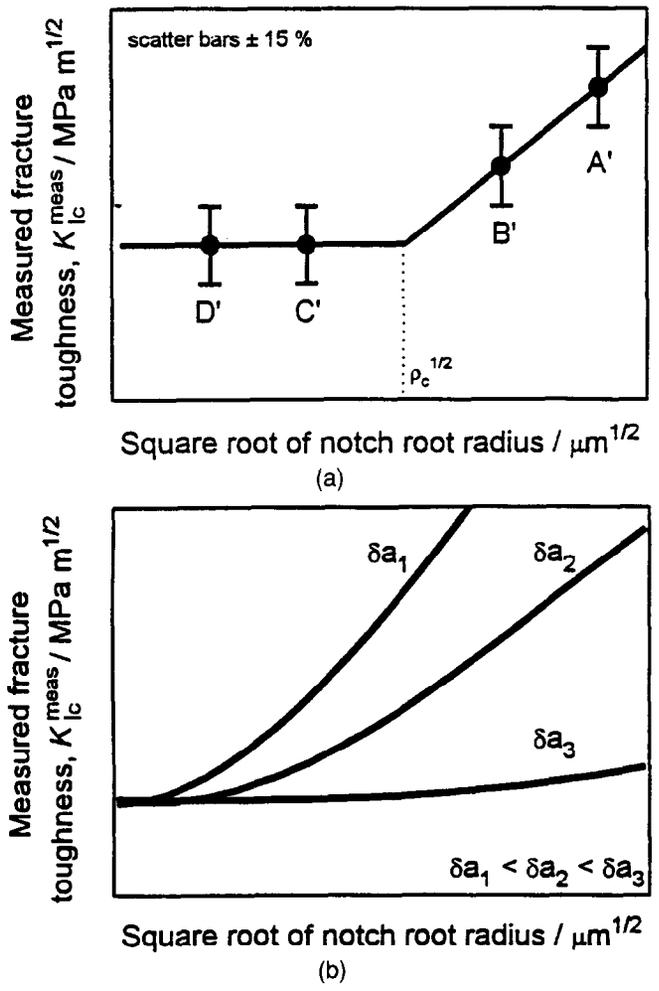

Fig. 5. (a) Schematic representation of the experimentally observed variation in fracture toughness, K_{Ic}^{meas} for constant starting crack size δa and varying notch-root radius ρ. (b) Schematic representation of the theoretical dependence of measured fracture toughness K_{Ic}^{meas} [as calculated from eqn (2)], on varying notch-root radius ρ for different sizes of a starting crack δa.

From eqn (4) X may be calculated as a function of ρ for any given Y and δa. It is clear that, unless δa is sufficiently large, a small crack will not experience a critical stress intensity factor at the same applied stress as would a long crack. It can be assumed that for any such small crack to see a critical stress intensity factor, the stress intensity experienced at the small crack tip must be K_{lsc} raised by $1/X$. Hence the variation in measured fracture toughness, K_{Ic}^{meas}, with increasing ρ may be calculated:

$$K_{Ic}^{meas} = \frac{K_T}{X} \tag{6}$$

where K_T is the true fracture toughness, K_{Ic}.

Relationship (4) may be rearranged so

$$\rho \approx \frac{4\ Y^2}{[\tanh^{-1} X]^2}\ \delta a \tag{7}$$

Then, in order to estimate the critical value of the notch root radius ρ_c, the assumption can be made that the X-ratio must reach a certain value before the method delivers constant results. However, since large scatter is usually observed in practice, there is little reason to demand that this ratio be unity. It should suffice to set X at a value between 0·9 and 0·95, in which case from eqn (6) it follows

$$\rho_c \approx A\ \delta a \tag{8}$$

where both A and δa are constants.

It is suggested here that in many cases δa is a feature of the microstructure, e.g. weakly bonded grain boundaries or large pores, etc. The determination of δa by microstructural analysis before mechanical testing thus enables the a priori

estimation of ρ_c, and gives an idea of the validity of the fracture toughness value determined.

Comparison with Experimental Data

To investigate the validity of eqns (4) and (6), SENB-S tests were made on small beam samples (b = 3 mm, w = 4 mm, L = 45 mm) of five ceramic materials: alumina (Al_2O_3); zirconia (ZrO_2); magnesia partially stabilized zirconia (MgPSZ); hot-pressed silicon nitride (HPSN); and sintered silicon carbide (SSiC). Notches were cut using high-speed rotary saws and diamond-tipped (diamond grit size between 15 and 25 μm) blades. The samples were tested in four-point bending at a load rate of 0·2 to 0·25 mm s^{-1}. The testing fixture was made of hardened steel and had freely movable rolls. The results of the tests are plotted in Figs 6 to 10.

The curves in Figs 6(b) to 10(b) were obtained by applying eqn (6). For any given values of δa and

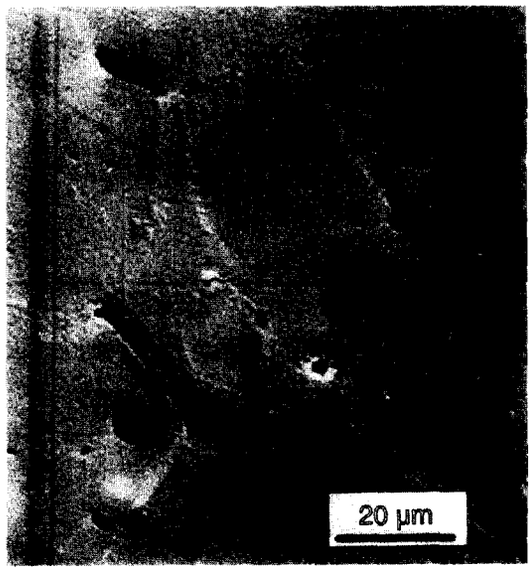

(a)

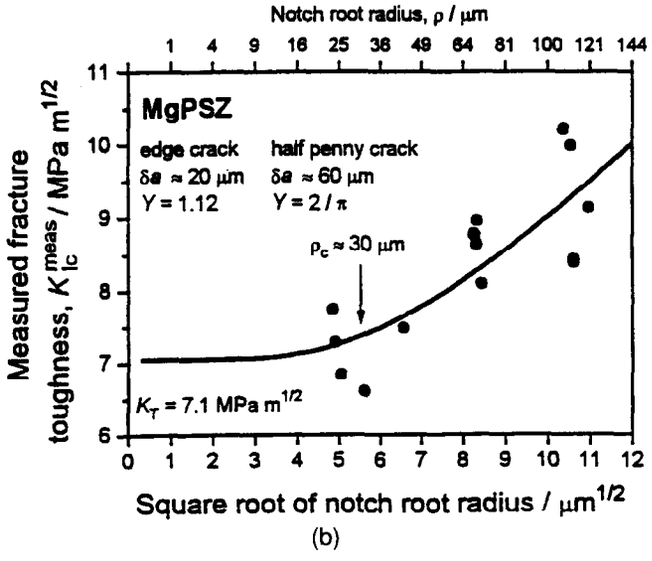

(b)

Fig. 6. (a) Microstructure of MgPSZ; (b) the best fit through the measured data points according to eqn (6).

(a)

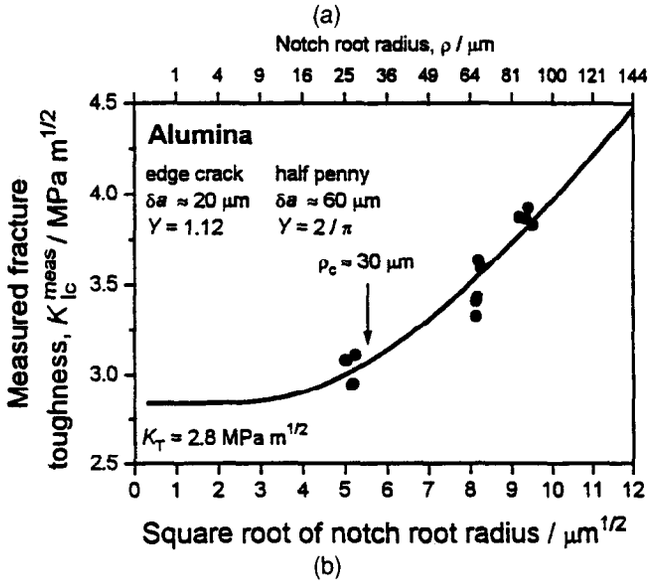

(b)

Fig. 7. (a) Microstructure of Al_2O_3; (b) the best fit through the measured data points according to eqn (6).

Y, the value of X follows from eqn (4) as a function of ρ. There are two possibilities to fix the parameters δa and Y, either by mathematical fitting or by microstructural analysis. The course of the curves may be determined by the product of Y^2 and δa, hence this has been used as one fitting parameter. By changing K_T the whole curve is shifted up or down. Both features have been used to get a reasonable fit to the experimental data points.

The parameters may also be fixed by microstructural analysis. The notch-tip small cracks were assumed to be related to some characteristic feature of the microstructure so δa was roughly approximated for each material on the basis of microstructural studies. Where no obvious suitable microstructural feature was found δa was assumed to be related to machining damage, e.g. the size of scratches from the diamond-tipped saw (approximately 10 μm). If isolated open grain boundaries or other obvious isolated defects in the microstructure

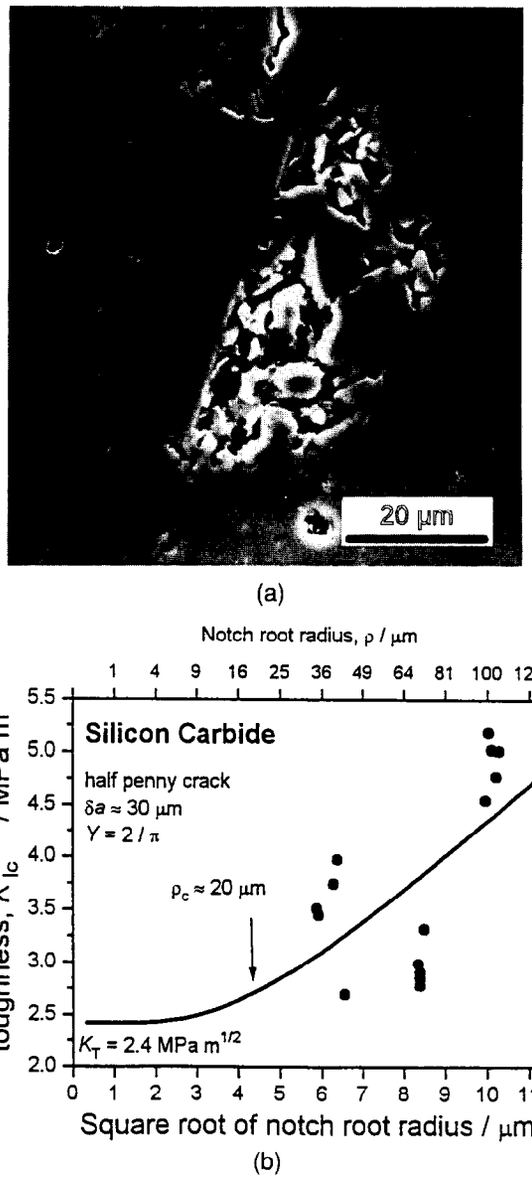

Fig. 8. (a) Microstructure of SSiC; (b) the best fit through the measured data points according to eqn (6).

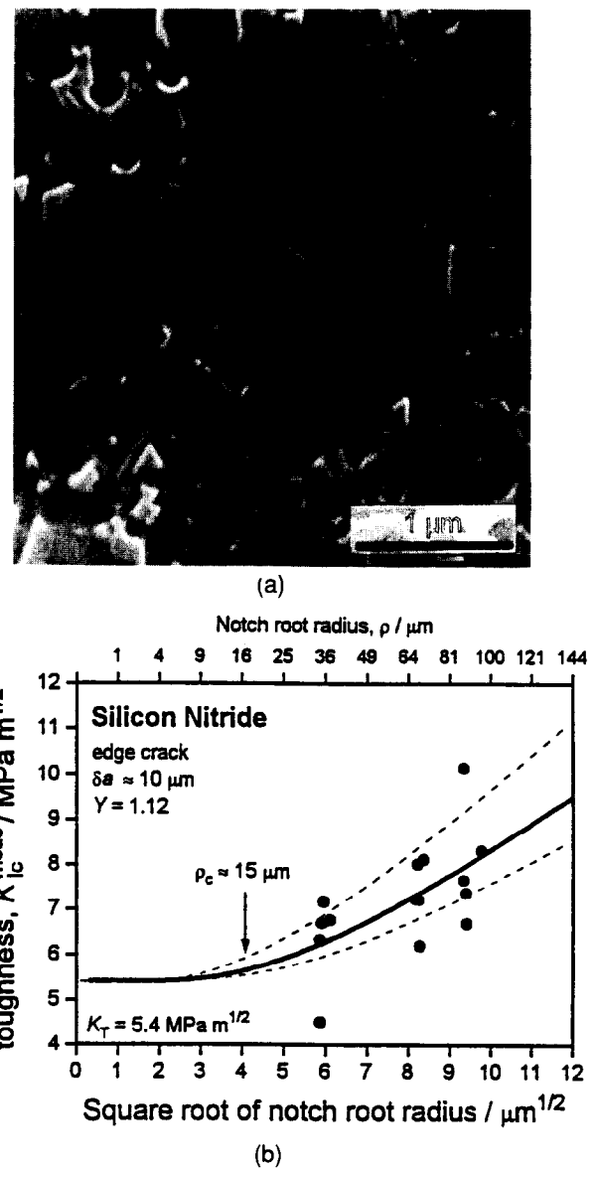

Fig. 9. (a) Microstructure of HPSN; (b) the best fit through the measured data points according to eqn (6) for scratches from diamond grit.

were observed, a half-penny crack configuration may be assumed for which $Y \approx 2/\pi$. If the spacing between defects is small or there is excessive porosity, an edge-crack configuration seems to be more plausible where $Y \approx 1{\cdot}12$. In reality any intermediate configuration is possible. The fitting procedure and the microstructural analysis yield similar results for the parameter $Y^2\,\delta a$ (within a factor of two).

The critical values of the notch root radii ρ_c shown in Figs 6(b) to 10(b) were estimated from eqn (8), by setting the value of X at 0·95, whereby A takes values of about 0·5 and 1·5 for half-penny or edge cracks, respectively.

Discussion of Results

Magnesia partially stabilized zirconia (MgPSZ)

The measurements on and the microstructures of MgPSZ are shown in Fig. 6. The mean grain diameter is about 40 μm. Some grain boundaries are badly sintered as is shown in Fig. 6(a). There are also regions where several open grain boundaries join giving a possible defect radius of 40 to 80 μm. The fitted curve in Fig. 6(b) gives a half-penny crack radius of 60 μm. However, the possibility of straight-through edge cracks cannot be completely excluded. To get the same curve for this notch-crack configuration a crack depth of 20 μm would be required, which correlates with a typical grain facet length. If it is assumed that one line of grain facets breaks open under the action of the sawing wheel, this would be the depth of the corresponding type edge crack. For this material the critical notch root radius is estimated to be about 30 μm and the measurements performed with the narrowest notch width (50 μm blade) are believed to be valid.

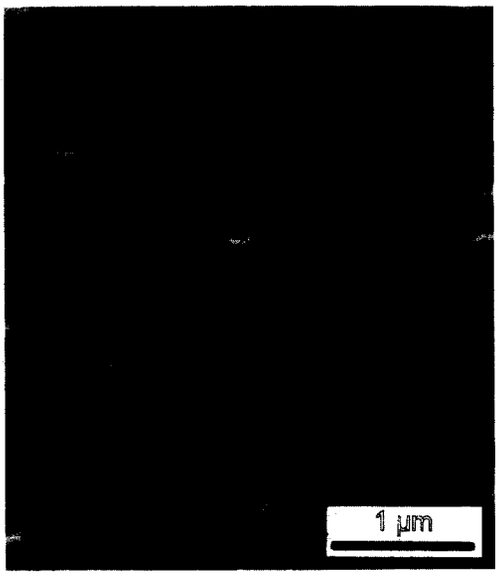

(a)

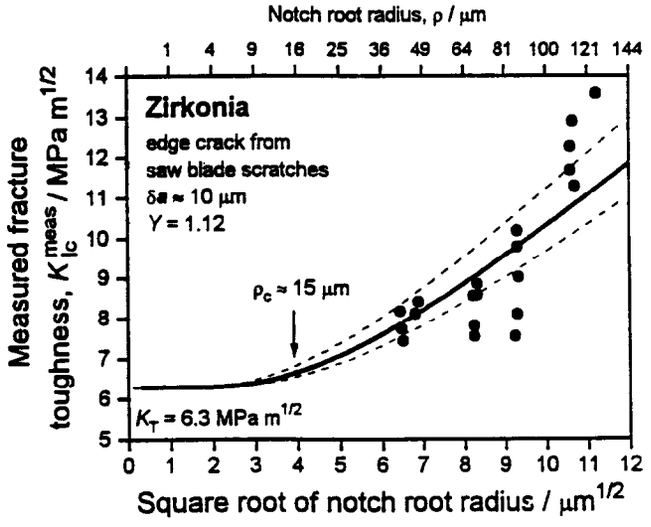

(b)

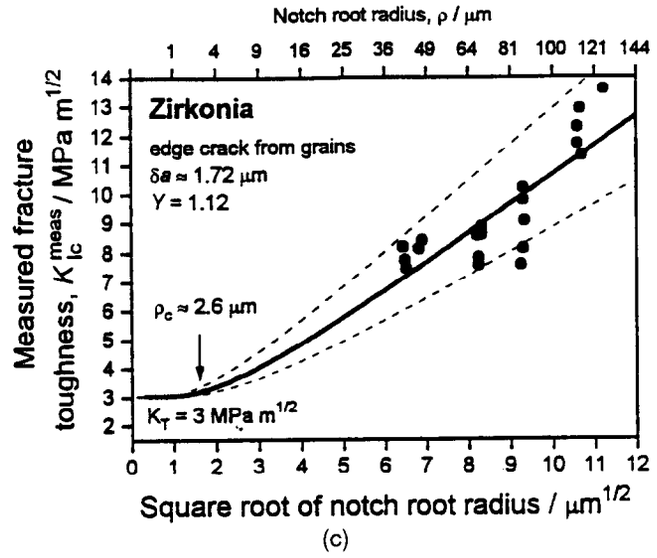

(c)

Fig. 10. (a) Microstructure of ZrO_2; (b) the best fit through the measured data points according to eqn (6) for the scratches from diamond grit; (c) the best fit through the measured data points according to eqn (6) for scratches as predicted by regressional fit. (The micrograph was provided courtesy of Dr F. Hoffer of the ZFE at the Forschungs Institut für Elektronenmikroscopie at the Technischeuniversität Graz, Austria.)

Alumina (Al_2O_3)

The results for alumina are shown in Fig. 7. The mean grain diameter is about 10 μm, and a lot of porosity was observed. The polishing also resulted in large amounts of grain breakout, even at the lowest loads used [see Fig. 7(a)]. It is assumed that such breakouts will also occur under the action of a saw. Both porosity and breakout would act together resulting in a more or less straight-through edge-type crack with a depth of about a few grain diameters .The best-fit curve in Fig. 7(b) is obtained for the through-thickness edge-crack configuration with a crack depth of 20 μm. An analogous fit for a half-penny shaped crack would require a crack depth of 60 μm, which does not seem to be justifiable from the microstructure. Again, the critical notch root radius is estimated to be about 30 μm and the measurements performed with the narrowest notch width (50 μm blade) are believed to be close to the true value.

Sintered silicon carbide (SSiC)

Sintered silicon carbide has a bi-modal microstructure consisting of isolated large grains (diameter of about 30 μm) embedded in a matrix of very fine grains (about 7 μm in diameter). Many fine pores are observed all over the material. Around the large platelet-like grains there is an exceptionally high level of porosity [see Fig. 8(a)], which is believed to be responsible for the fracture-initiating crack. The fitted curve in Fig. 8(b) gives a depth of 30 μm for a half-penny crack, which corresponds exactly to the observed feature. Due to the relatively small defect size the critical notch-root radius is determined to be only 20 μm and all the measured values should be too high.

However, one set of values [as shown in Fig. 8(b)] seems to agree with the theoretically predicted true fracture toughness. This set of tests was carried out using different apparatus from the other two sets. If this apparatus was slightly misaligned a slight hammering action could result. This would cause an increased crack size or a different crack geometry, both of which would result in lower apparent K_{Ic}.

Hot-pressed silicon nitride (HPSN)

The HPSN used has a very fine grain structure, the grain morphology of which is shown in Fig. 9(a). Needle-like grains, up to 3 μm in the long axis, were observed. Microstructural analysis revealed no obvious features that could be thought of as fracture-initiating defects. It may be assumed that scratches from the saw blade act as starting cracks. The size of the diamond saw grit was between 15 and 30 μm, so the depth of the resulting scratches would therefore be about half this size

(between about 7 and 15 μm). The value of δa predicted by the mathematical fit of eqn (7) shown in Fig. 9(b) seems to support this assumption. However, the prediction cannot be seen as definitive due to the large experimental data scatter.

The critical notch-root radius is small, about 15 μm. The measured values were therefore all too high. The large scatter in measured values may possibly be explained if the initial starting crack size is varied between the smallest assumed crack and the largest assumed crack, from about 7 to about 15 μm respectively. The dashed lines in Fig. 9(b) show the scatter band that could be expected from such a variation in starting crack size.

Zirconia (ZrO_2)

The microstructure of zirconia shown in Fig. 10(a) is very fine. The grains are equiaxed and generally less than 1 μm in size; a reasonable amount of porosity was observed, but nothing much larger than the grains. No obvious microstructural feature that acts as a fracture-initiating crack could be observed. The same assumption could be made as in case of HPSN, i.e. that the starting cracks are the scratches from the saw blade of about 10 μm [see Fig. 10(b)]. As before, the scatter band describes the variation in scratch depth resulting from the varying diamond grit size.

Although the data are described properly by the fit above, a slightly better fit may be achieved by mathematical regression [Fig. 10(c)]. The regression suggests a starting crack of about 1·7 μm. The dashed lines here represent the scatter resulting from varying the starting crack size by about one grain diameter. It should, however, be noted that this regression also yields a K_T that is very low. In indentation experiments no cracks at all were seen, even at indentation loads of 30 kg. This would indicate a much higher fracture toughness.

In both cases the fit quality is not very high and a clear distinction between the two cannot be made from the mathematical point of view.

Conclusions

In general, the SENB-S method of fracture toughness testing is reliable, easily applicable and shows low scatter both within and between laboratories. However, the appearance of the critical notch-root radius effect is unavoidable. Therefore, to obtain valid and consistent results it is imperative to cut suitably thin notches.

The notch-root radius effect may be explained if the fracture-initiating crack is assumed to be some small crack in front of the notch tip, under the influence of the stress interaction field of the notch. The theory presented shows that the values of K_{Ic} are valid only if the notch thickness is below some critical value, ρ_c. The magnitude of ρ_c is shown to be proportional to the size of the critical, fracture-initiating defect. The proportionality factor depends on the defect geometry but is of the order of unity. Equation (8) presented in this paper enables the a priori estimation of ρ_c if microstructural studies can reveal an appropriate defect-like microstructural feature. If no such feature can be found, the lower limit of defect size, i.e. machining scratches of about 10 μm, may be adopted.

For coarse-grained materials (of diameter about 50 μm) there will always be some defects (e.g. open grain boundaries or broken grains) of the order of magnitude of the grain size. Therefore it is possible with simple contemporary technology to make notches thin enough to obtain valid measurements from these materials. The same is true for materials containing a reasonable number of large defects (diameter of about 50 μm or more).

However, for materials with very fine and clean microstructures, the starting defects are most probably machining scratches and more advanced technology or methodology will be required to make notches thin enough to deliver valid results.

Acknowledgement

This work was supported by the Ministerium für Wissenschaft und Forschung der Republik Österreich under the contract no. Gz 49·929/3-II/4/94, Mechanische Eigenschaften keramische Hochleistungswerkstoffen.

References

1. Primas, R. J. & Gstrein, R., ESIS TC6 round robin on fracture toughness (Draft Nov. 1994). EMPA Report No. 155'088, Eidgenössische Materialprüfungs- und Forschungsanstalt, Dübendorf, Switzerland, 1994.
2. Amin, K. E., *Toughness, Hardness and Wear*, Engineered Materials Handbook: Vol. 4 Ceramics and Glasses. ASM International, Metals Park, OH, 1991, pp. 599–609.
3. Munz, D. & Fett, T., *Mechanisches Verhalten keramischer Werkstoffe: Versagensablauf, Werkstoffauswahl, Dimensionierung*. Springer-Verlag, Berlin, 1989.
4. Bertolotti, R. L., Fracture toughness of polycrystalline Al_2O_3. *J. Am. Ceram. Soc.*, **56**[2] (1973) 107.
5. Nishida, T., Hanaki, Y. & Pezzotti, G., Effect of notch-root radius on the fracture toughness of a fine-grained alumina. *J. Am. Ceram. Soc.*, **77**[2] (1994).
6. Schwalbe,K.-H., *Bruchmechanik metallischer Werkstoffe*. Carl Hanser Verlag, München–Wien, 1980.
7. Fett, T., Stress intensity factors and weight functions for cracks in front of notches. KfK 5254, Kernforschungszentrum Karlsruhe, Karlsruhe, Germany, 1993.